T_1 dependence of magnetization transfer effect for macromolecules

Poster No.: C-0827

Congress: ECR 2017

Type: Scientific Exhibit

Authors: T. Sasaki[1], Y. Kanazawa[1], Y. Matsumoto[1], H. Hayashi[2], N. Ikemitsu[1], T. Usuda[1], M. Miyoshi[3], M. Harada[1]; [1]Tokushima/JP, [2]Tokushima, Tokushima/JP, [3]Hino/JP

Keywords: Molecular, genomics and proteomics, Image verification, Physics, Molecular imaging, Imaging sequences, MR-Functional imaging, MR, Radiation physics, MR physics, Hybrid Imaging, Tissue characterisation

DOI: 10.1594/ecr2017/C-0827

Aims and objectives

Magnetization transfer (MT) is a cross relaxation phenomenon in which the proton is able to move freely; known as bulk water and bound water. The MT effect is observed and provides the signal attenuation for the MT pulse; then, a RF pulse is added at an off-resonance frequency. This method is said to be the off-resonance method. Signal attenuation occurred for MT pulse by interaction between bulk water and bound water e.g., spin exchange, and chemical shift. The magnetization transfer contrast (MTC) method is demonstrated as the above phenomenon [1, 2]. Mainly, the MTC method is used for magnetic resonance angiography (MRA), of which the clinical application to the head has many advantages; such as signal saturation of the background on a target tissue, e.g., detection of blood. There is one report that the observation of the peripheral artery in the brain had improved by signal-attenuation on the substance of the background by addition of a MT pulse [3]. Additionally, there are some reports about the application of MTC to cartilage macromolecules such as the collagen [4].

Generally, a magnetization transfer ratio (MTR) is known to be an index to express signal attenuation by the MT effect quantitatively [6]. MTR is calculated by the ratio of the remainder of each image without and with a MT pulse. Spin exchange between bulk water and bound water is an important attenuation factor. The spin exchange rate depends on T_1 which has been reported by Henkelman [5].

For T_1 calculation methods, there are the inversion recovery (IR) method and variable flip angle (VFA) method. The IR method is used as the gold-standard method for T_1 calculation. On the other hand, the VFA method is performed using a spoiled gradient-echo (SPGR) sequence in general, which makes it possible to be a faster imaging method than the IR method. At high magnetic field strengths, the VFA method is sensitive to B_1 inhomogeneity [7, 8]. Accordingly, B_1 inhomogeneity needs to be corrected.

It is important that we evaluate how much effect T_1 has on the MT of macromolecules. However, little attention has been given to the direct measurement of T_1 and the effect it has on the MT. To assess the relationship between T_1 and the MT effect on macromolecules, we constructed a T_1 map using the variable flip angle (VFA) method with a MT pulse.

Methods and materials

We performed a phantom experiment. The phantom was created using a set of six samples in a cylindrical vessel. The sample components used were deionized water with

polyethylene glycol (PEG) macromolecules at different concentrations (0, 10, 20, 30, 40, and 50 wt%). Figure 1 shows the schematics of the phantom used in this study.

All imaging analysis were applied using an in-house program, MATLAB (Mathworks, Natick, MA, USA). A chart of the procedure of this study is shown in Fig. 2.

1. MR imaging

On a 3.0 T MR scanner system (Discovery MR750, GE Healthcare, Waukesha, WI, USA), MR imaging data of the phantom were acquired with spoiled gradient echo (SPGR) sequence with and without a MT pulse (offset frequency = 800, 1200, 1600 Hz). Table 1 shows detailed imaging parameters.

2. B_1 correction

The B_1 map was derived using the double angle method. The method uses the MR images at two flip angles (FA) acquired by gradient echo (GRE) sequence. The MR images for B_1 mapping were acquired using 2 second repetition time (TR), 5.8 ms echo time (TE), 40 degrees FA #, 80 degrees FA 2#, and 5 mm slice thickness. Table 2 shows detailed imaging parameters for B_1 mapping. B_1 map was constructed using the following equation [9]

$$B_1^{flip\ angle} = \arccos\left(\frac{S_{2\alpha}}{2S_\alpha}\right)$$

Fig. 3: Equation(1).
References: - Tokushima/JP

where $S_{\#}$ and $S_{2\#}$ are the signal intensities of the # and 2# FA images. Using equation (1), we created a B_1 map from the MR images. Then, we applied the B_1 map to MR imaging data, and performed B_1 correction.

3. T_1 mapping

After B_1 correction was performed, T_1 maps were derived using the VFA method. The VFA method uses more than two FA images acquired by SPGR sequence. Signal intensities of SPGR sequence are given by [7,10]

$$S_{SPGR} = M_0 \sin\alpha \frac{1 - exp\left(\frac{-TR}{T_1}\right)}{1 - exp\left(\frac{-TR}{T_1}\right)\cos\alpha}$$

Fig. 4: Equation(2).
References: - Tokushima/JP

where TR and FA # are the control parameters varied by the operator, M_0 is the equilibrium magnetization, SSPGR is the measured signal values. Then, based on equation (2), we performed T_1 fitting as follow:

$$[M_0\ T_1] = \arg\min\left(\sum_{i=1}^{N_{SPGR}} \left(S_{SPGR,i} - S_{SPGR,i}(\alpha_i)\right)^2\right)$$

Fig. 5: Equation(3).
References: - Tokushima/JP

where N_{SPGR} is the number of varied FA, arg min f(x) is the function for which f(x) attains the smallest value, M_0 and T_1 are the estimated parameters determined by nonlinear curve fitting. Initial estimation values M_0 and T_1 from the curve fitting values were set to the maximum signal intensity in the same pixel of images and 2000 ms, respectively. With fixed TR and variable FAs, the optimization of the parameters M_0 and T_1 was calculated according by the relationship between signal intensity and FA. Mean T_1 values and standard division (SD) of all samples were measured on T_1 maps.

4. MTR mapping

MTR maps were calculated individually using two FA images with and without a MT pulse. MTR is determined by [2]

$$MTR = \frac{S_0 - S_{SAT}}{S_0}$$

Fig. 6: Equation(4).
References: - Tokushima/JP

where S_0 and S_{SAT} are signal values with and without a MT pulse. MTR of all samples were measured on MTR maps at each FA and offset frequency.

Images for this section:

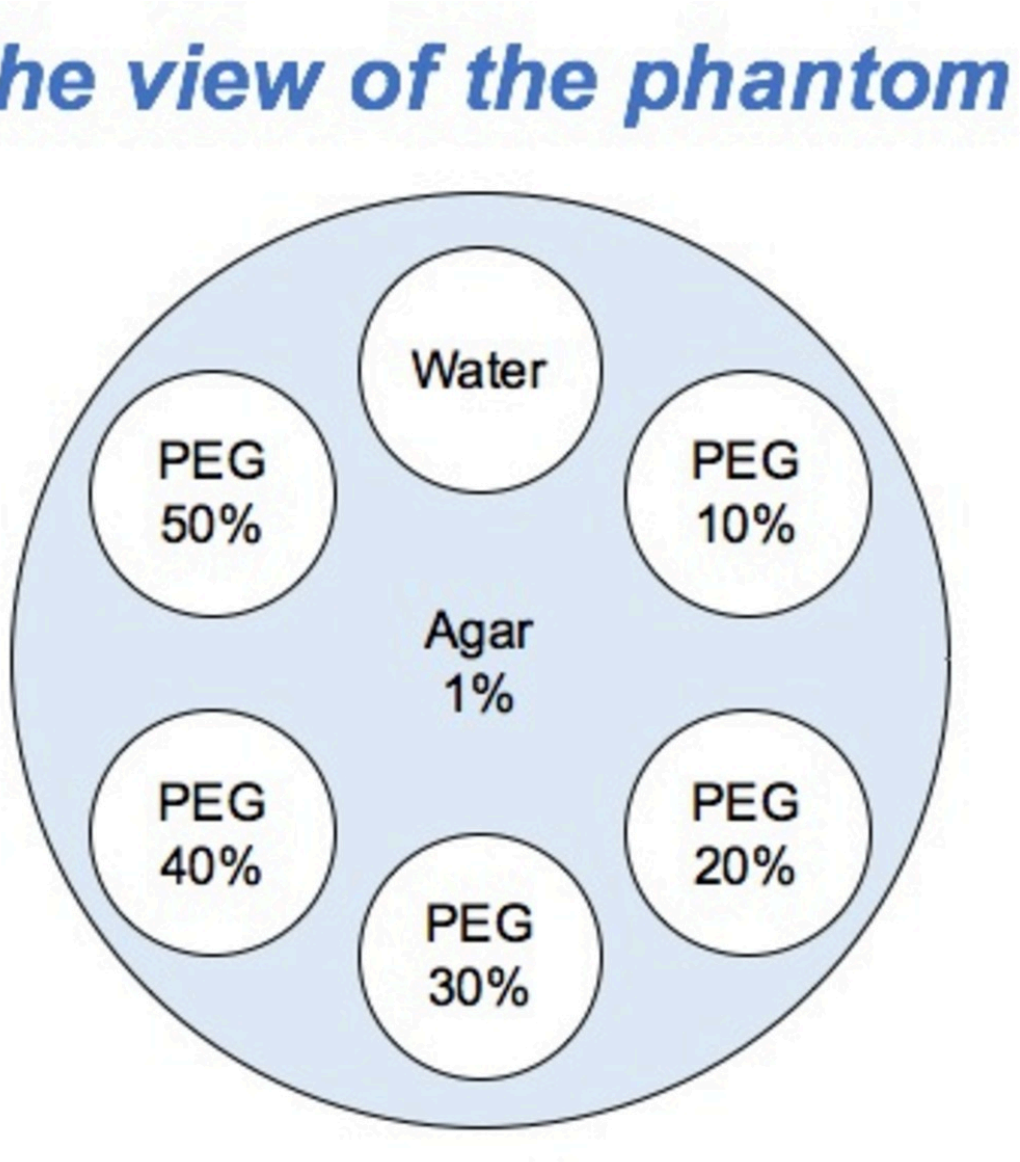

Fig. 1: The schematics of the phantom.

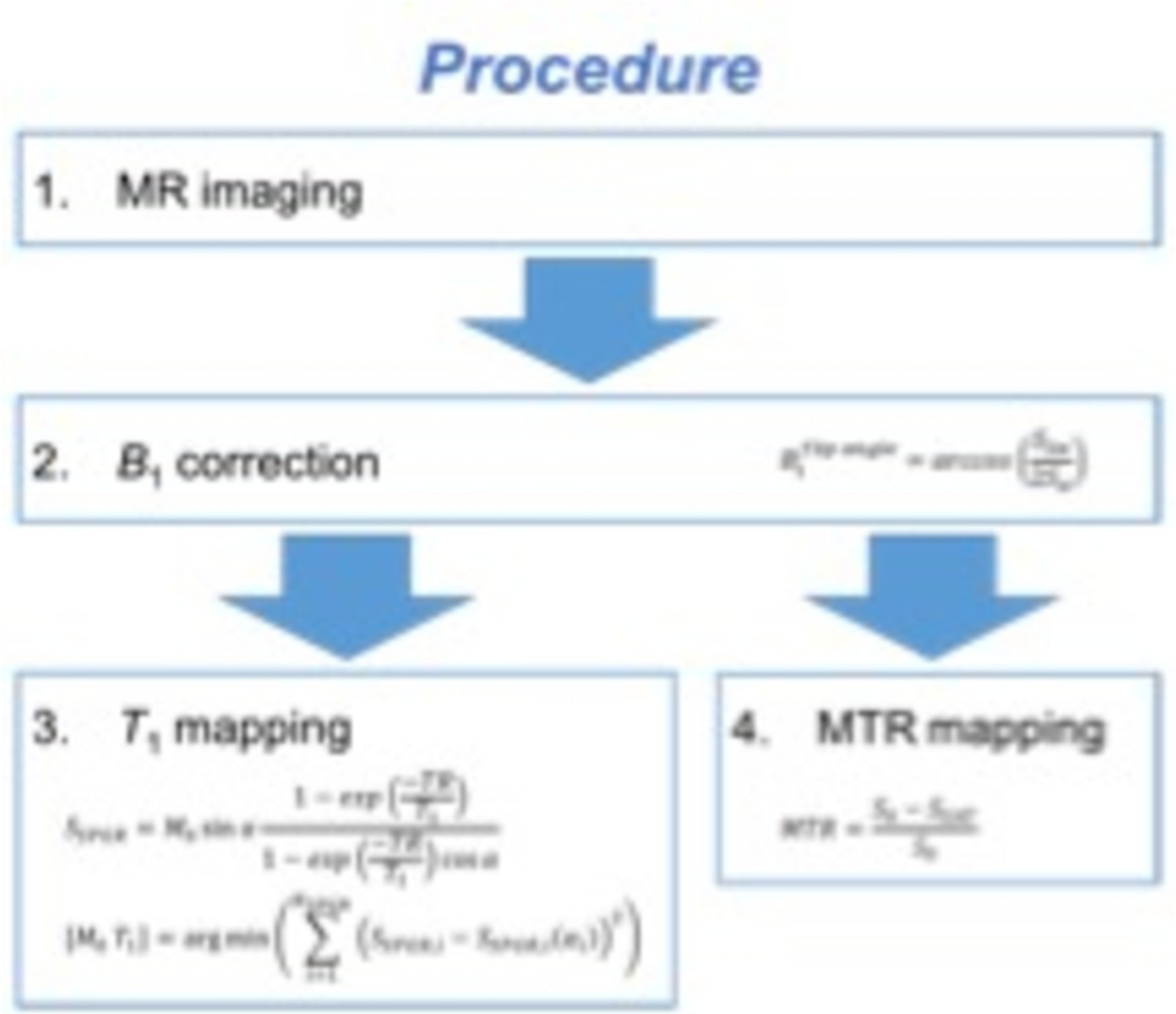

Fig. 2: Chart of the procedure.

Imaging parameters	Setting values
Sequence	Spoiled GRE (SPGR)
Repetition time (TR) [ms]	600
Echo time (TE) [ms]	5.8
Flip angle (FA) [degree]	5, 20, 40, 60, 90
MT pulse [Hz]	800, 1200, 1600
Slice thickness [mm]	5

Table 1: Imaging parameters for T1 and MTR mappings.

Imaging parameters	Setting values
Sequence	Gradient echo (GRE)
TR [ms]	2000
TE [ms]	5.8
FA [degree]	40, 80
Slice thickness [mm]	5

Table 2: Imaging parameters for B1 mappiing

Results

Table 3 shows the relationship between PEG concentrations and mean T_1 values of each sample with and without a MT pulse.

Figure 7 shows T_1 map derived from the VFA method with and without a MT pulse (Off-set frequency: 800, 1600 Hz).

Figure 8 shows a graph of the data, Table. 3. By the addition of MT pulse, the change in T_1 values was seen, but there were almost no changes caused by differences in offset frequency of the MT pulse. In the PEG 30% solution, a change in the T_1 value by the MT pulse addition was not seen. A decreasing tendency in T_1 values was seen at lower PEG concentrations, but the T_1 values showed an increasing tendency when PEG concentration exceeded 30%.

Figure 9 shows the relationship between PEG concentrations and MTR at each FA (5, 20, 40, 60, and 90 degrees). In MTR, the influence of FA and offset frequency was remarkable.

Images for this section:

PEG concentration [%]	T_1 values [ms]			
	MT off	MT800Hz	MT1200Hz	MT1600Hz
0	2039 ± 126	1886 ± 34	1926 ± 26	1909 ± 27
10	1914 ± 36	1817 ± 28	1834 ± 26	1823 ± 27
20	1771 ± 28	1728 ± 31	1731 ± 32	1723 ± 32
30	1649 ± 32	1644 ± 35	1646 ± 40	1642 ± 39
40	1490 ± 47	1546 ± 42	1537 ± 48	1531 ± 47
50	1200 ± 278	1322 ± 108	1310 ± 123	1300 ± 152

Table 3: The measured T1 values.

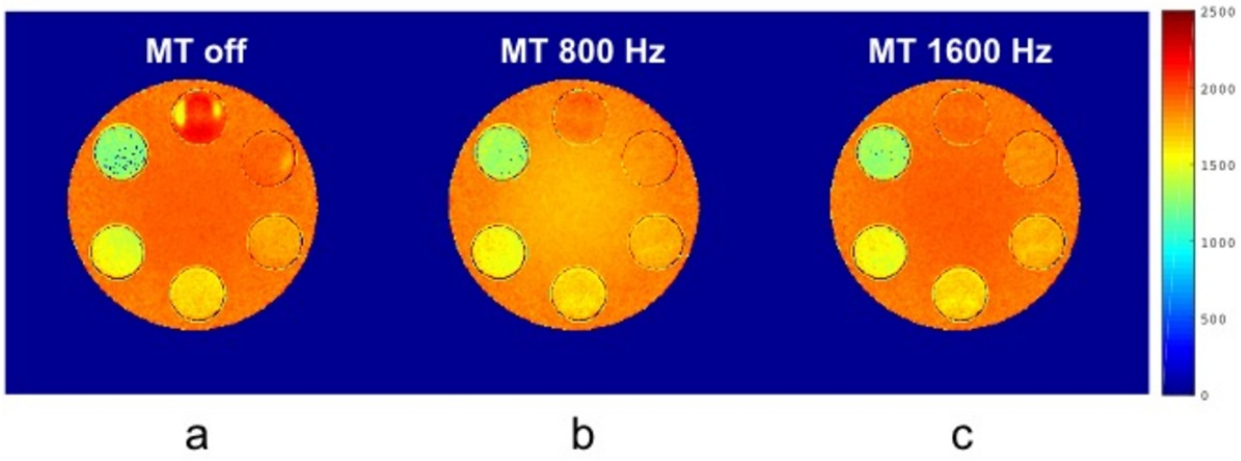

Fig. 7: T1 map derived from the VFA method with and without a MT pulse (Off-set frequency: 800, 1600 Hz).

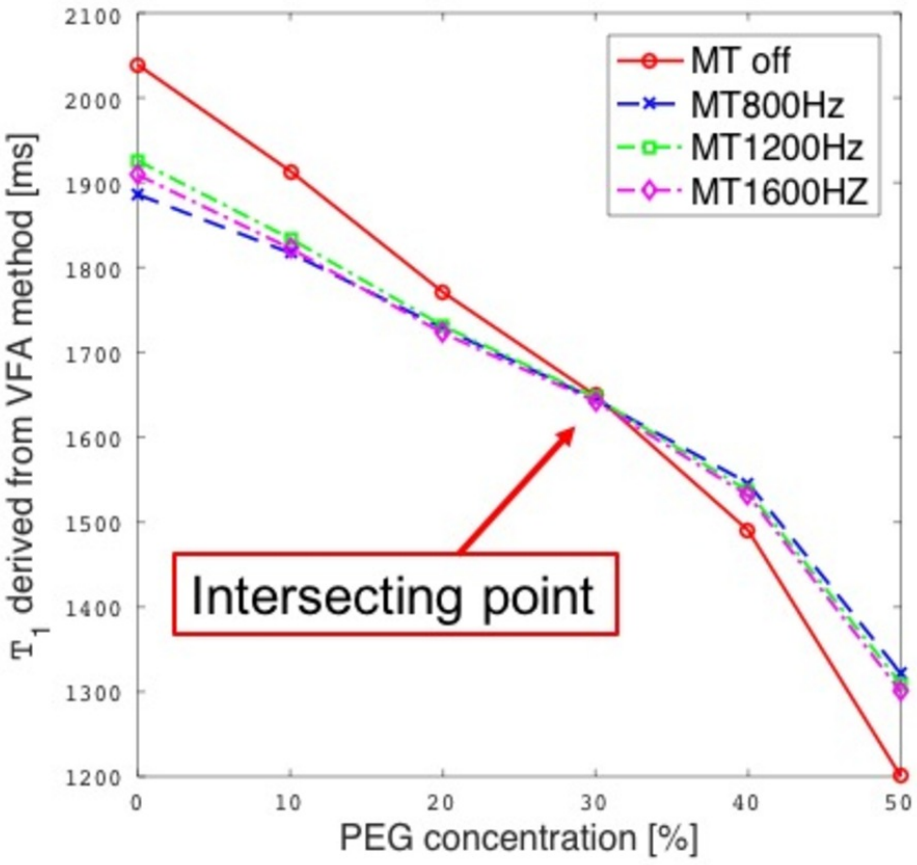

Fig. 8: The relationship between PEG concentrations and measured T1 values.

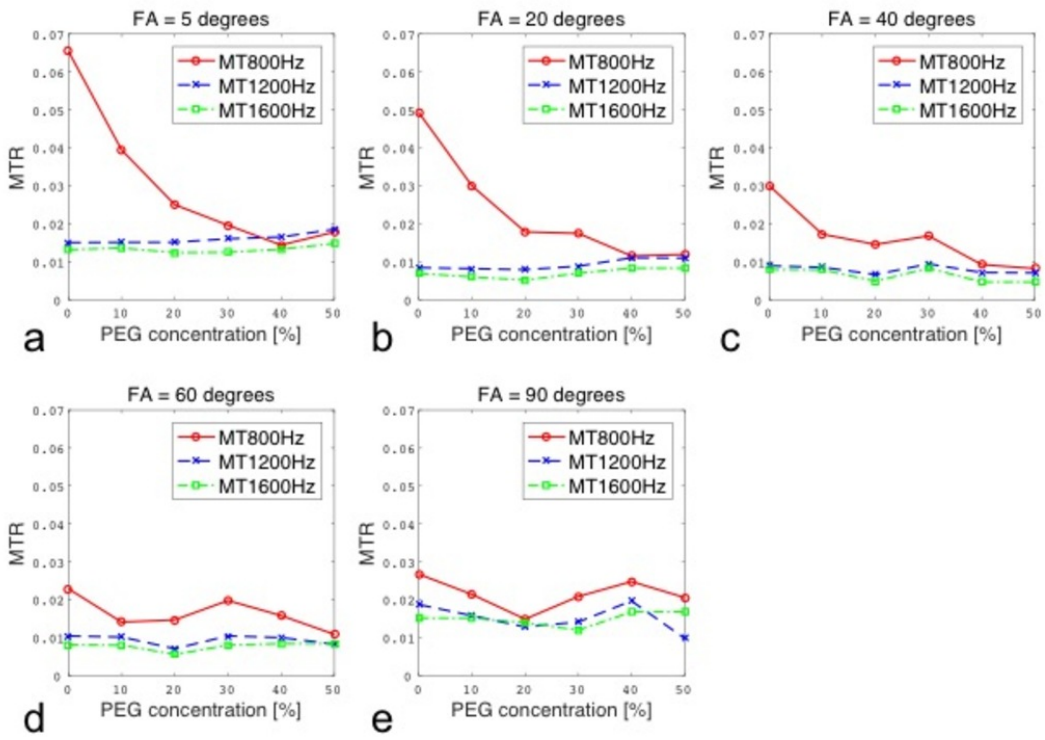

Fig. 9: The relationship between PEG concentrations and MTR at each FA (5, 20, 40, 60, and 90 degrees).

© - Tokushima/JP

Conclusion

Determination of T_1 with a MT pulse makes it possible to obtain more detailed information of macromolecules not provided when using MTR.

Personal information

Author Names:

Toshiaki Sasaki[1], Yuki Kanazawa[2], Yuki Matsumoto[1], Hiroaki Hayashi[2], Natsuki Ikemitsu[1], Takatoshi Usuda[1], Mitsuharu Miyoshi[3], and Masafumi Harada[2]

Author Affiliations:

1. School of Health Sciences, Tokushima University

2. Institute of Biomedical Sciences, Tokushima University Graduate School

3. MR Applications and Workflow Asia Pacific GE Healthcare Japan Corporation

Corresponding Author and Reprint Info:

Yuki Kanazawa, PhD

Institute of Biomedical Sciences, Tokushima University Graduate School

3-18-15, Kuramoto-Cho, Toksuhima City, Tokushima, 770-8509, Japan

E-mail: yk@tokushima-u.ac.jp

References

1. Wolff SD, Balaban RS. Magnetization transfer contrast (MTC) and tissue water proton relaxation in vivo. Magn Reson Med. 1989;10(1):135-144
2. Henkelman RM, Stanisz GJ, Graham SJ. Magnetization transfer in MRI: a review. NMR Biomed. 2001;14(2):57-64.
3. Edelman RR, Ahn SS, Chien D, Li W, Goldmann A, Mantello M, Kramer J, Kleefield J. Improved time-of-flight MR angiography of the brain with magnetization transfer contrast. Radiology. 1992;184(2):395-399.

4. Wolff SD, Chesnick S, Frank JA, Lim KO, Balaban RS. Magnetization transfer contrast: MR imaging of the knee. Radiology. 1991;179(3):623-628.
5. Henkelman RM, Huang X, Xiang QS, Stanisz GJ, Swanson SD. Quantitative interpretation of magnetization transfer. Magn Reson Imag. 1993;29(6):759-766.
6. Finelli DA, Reed DR. Flip angle dependence of experimentally determined T1sat and apparent magnetization transfer rate constants. Magn Reson Imag. 1998;8(3):548-553.
7. Hurley SA, Yarnykh VL, Johnson KM, Field AS, Alexander AL, Samsonov AA. Simultaneous variable flip angle-actual flip angle imaging method for improved accuracy and precision of three-dimensional T1 and B1 measurements. Magn Reson Med. 2012;68(1):54-64.
8. Collins CM, Li S, Smith MB. SAR and B1 field distributions in a heterogeneous human head model within a birdcage coil. Magn Reson Med. 1998;40(6):847-856.
9. Sacolick LI, Wiesinger F, Hancu I, Vogel MW. B1 mapping by bloch-siegert shift. Magn Reson Med. 2010;63(5):1315-1322.
10. Kanazawa Y, Hayashi H, Harada M. Clinical approach of T1-mapping for hemodynamic analysis. Med Imag & Infor Sci. 2015;32(4).